Assessing the role of hematopoietic plasticity for endothelial and hepatocyte development by non-invasive lineage tracing

Matthias Stadtfeld and Thomas Graf*

Department of Developmental and Molecular Biology, Albert Einstein College of Medicine, 1300 Morris Park Avenue, Bronx, NY 10461, USA

*Author for correspondence (e-mail: graf@aecom.yu.edu)

Accepted 29 October 2004

Development 132, 203-213
Published by The Company of Biologists 2005
doi:10.1242/dev.01558

Summary

Hematopoietic cells have been reported to convert into a number of non-hematopoietic cells types after transplantation/injury. Here, we have used a lineage tracing approach to determine whether hematopoietic plasticity is relevant for the normal development of hepatocytes and endothelial cells, both of which develop in close association with blood cells. Two mouse models were analyzed: vav ancestry mice, in which essentially all hematopoietic cells, including stem cells, irreversibly express yellow fluorescent protein (YFP); and lysozyme ancestry mice, in which all macrophages, as well as a small subset of all other non-myeloid hematopoietic cells, are labeled. Both lines were found to contain YFP$^+$ hepatocytes at similar frequencies, indicating that macrophage to hepatocyte contributions occur in unperturbed mice. However, the YFP$^+$ hepatocytes never formed clusters larger than three cells, suggesting a postnatal origin. In addition, the frequency of these cells was very low (~1 in 75,000) and only increased two- to threefold after acute liver injury. Analysis of the two mouse models revealed no evidence for a hematopoietic origin of endothelial cells, showing that definitive HSCs do not function as hemangioblasts during normal development. Using endothelial cells and hepatocytes as paradigms, our study indicates that hematopoietic cells are tightly restricted in their differentiation potential during mouse embryo development and that hematopoietic plasticity plays at best a minor role in adult organ maintenance and regeneration.

Key words: Hematopoietic plasticity, Hepatocyte development, Endothelial cell development, Hematopoietic stem cells, Lineage tracing

Introduction

A central tenet of developmental biology states that every cell type in the animal can be assigned to one of the primordial germ layers ectoderm, mesoderm and endoderm. Within the adult, different stem cells are responsible for the maintenance of tissues such as blood, the epidermis of the skin or the epithelial layer of the gut. These cells are thought to be restricted in their developmental potential. However, nuclear transfer experiments showed that differentiation is an epigenetic process that can be reversed in principle (Gurdon and Byrne, 2003; Hochedlinger and Jaenisch, 2002). Furthermore, some vertebrate cells are naturally endowed with developmental plasticity, such as neural crest cells, which despite their ectodermal origin, give rise to muscle, cartilage and bone, all of which are normally derived from mesoderm (Garcia-Castro and Bronner-Fraser, 1999).

Based on transplantation experiments into irradiated hosts, it has been proposed that hematopoietic stem cells (HSCs) also possess developmental plasticity and can trans-differentiate into cells of all three germ layers (Graf, 2002; Herzog et al., 2003; Wagers and Weissman, 2004). Two non-hematopoietic cell types for which this has been documented after transplantation of single HSCs are hepatocytes and endothelial cells (Camargo et al., 2004; Grant et al., 2002). Hepatocytes are the progeny of hepatoblasts, endodermal derivatives specified in the mouse around midgestation (Zaret, 2002), which co-localize with HSCs to the fetal liver (Godin and Cumano, 2002; Suzuki et al., 2000). In FAH-deficient mice, a well-studied model of chronic liver failure (Lagasse et al., 2000), blood to liver conversions have been shown to be mediated by fusion of macrophages with hepatocytes (Camargo et al., 2004; Willenbring et al., 2004). However, direct trans-differentiation of HSCs into hepatocytes has recently been reported for wild-type mice following liver injury and HSC transplantation (Jang et al., 2004). Finally, after transplantation of human HSCs into fetal sheep, as much as 20% of hepatocytes were reported to be of donor origin (Almeida-Porada et al., 2004).

Endothelial cells, like hematopoietic cells, are of mesodermal origin. The development of these two cell types, which share the expression of several marker genes, is regulated by overlapping sets of transcription factors (Bloor et al., 2002; Ema et al., 2003; Oettgen, 2001). Definitive HSCs arise from vascular endothelial cells of the dorsal aorta (de Bruijn et al., 2002; Jaffredo et al., 1998; Nishikawa et al., 1998). A common precursor of endothelial and hematopoietic cells, the hemangioblast, has been identified in embryonic stem cell cultures (Choi et al., 1998), further underscoring the close

relationship of these two lineages. Recently, it has been reported that fetal as well as adult HSCs transplanted into irradiated hosts can generate endothelial cells and thus appear to function as hemangioblasts (Bailey et al., 2004; Grant et al., 2002; Tamura et al., 2002).

These studies raise the possibility that hematopoietic contributions to hepatocytes and endothelial cells occur as normal development processes. This may happen particularly in the fetal liver where hematopoiesis, vasculogenesis and hepatocyte differentiation coincide. Alternatively, hematopoietic plasticity might also play a role in adults as a mechanism of tissue maintenance (Blau et al., 2001). To test these possibilities, we designed a mouse model based on Cre/loxP technology in which essentially all hematopoietic cells, including fetal and adult HSCs, are irreversibly labeled by YFP expression ('vav ancestry mice'). We analyzed the hepatocyte and endothelial cell compartment of these mice in comparison with lysozyme ancestry mice, in which most myelomonocytic cells and to a lesser degree all other adult hematopoietic cell types, including HSCs, irreversibly express YFP (Ye et al., 2003).

Materials and methods

Constructs

A plasmid containing the HS21/45 *vav* regulatory elements was obtained from Dr Jerry Adams (Melbourne). The human CD4 cassette in this plasmid (Ogilvy et al., 1999) was exchanged with a bicistronic sequence coding for Cre recombinase and YFP linked by an IRES element (Clontech, Palo Alto, CA), using the *Not*I and *Sfi*I restriction sites. The vav-Cre cassette was then integrated between two repeats of the 250 bp core element from the chicken β globin insulator (Recillas-Targa et al., 2002). The transgenic construct was linearized by *Xho*I and *Sac*II digestion and injected into oocytes at the AECOM Transgenic Mouse Facility. Details of the cloning procedure and plasmid maps can be obtained on request.

Mice

PCR primers used to identify mice containing vav-Cre were: 5′-CC-ATGGCACCCAAGAAGAAG-3′ (Vav1) and 5′-GCTTAGTTTTCC-TGCAGCGG-3′ (Vav2), which give a product of 2.6 kb that spans from the start codon of Cre to the stop codon of YFP. PCR reactions were carried out with 100 ng of tail DNA for 35 cycles (30 seconds denaturation at 94°C, 60 seconds annealing at 60°C and 150 seconds elongation at 72°C) and the products analyzed on a 1.5% agarose gel. Vav ancestry mice were obtained by crossing vav-Cre transgenic mice with ROSA26R-lacZ and ROSA26R-YFP reporter mice, respectively (Soriano, 1999; Srinivas et al., 2001). The phenotypes of the offspring were determined by examining ear clips under a Nikon Eclipse E600 fluorescence microscope equipped with a filter to visualize YFP (Chroma Technology, Rockingham, VT #41028). Mice with YFP^+ cells of dendritic morphology were identified as 'vav ancestry mice'; mice with patches of YFP^+ non-hematopoietic cells as 'chimeric control mice'; and mice with no YFP^+ cells as negative control mice. To obtain mice homozygous for the reporter gene, female vav ancestry mice were crossed with ROSA26R males. The lysozyme ancestry mice used for this study were homozygous for ROSA26R-YFP and either homozygous or heterozygous for LysM-Cre. They were genotyped as described (Ye et al., 2003). Mice were bred and maintained in accordance with guidelines from the Institute for Animal Studies of the Albert Einstein College of Medicine.

Bone marrow reconstitution

Mononucleated bone marrow cells from vav ancestry mice were prepared by sterile flushing of the tibia and femur bones as described before (Ye et al., 2003). A sample of these cells (2×10^6) was injected into the tail vein of non-transgenic littermates lethally irradiated with two doses of 600 rad in the 24 hours before the transplantation. The degree of donor engraftment was determined by flow cytometry of peripheral blood cells 4 weeks after transplantation and at the time when the animals were sacrificed (all mice used in this study had a donor contribution of at least 90% and 95% at these two time points, respectively).

Liver injury

Adult mice were injected intraperitoneally with a single dose of carbon tetrachloride (CCl_4) solution (10 μl per 3 g bodyweight of a 30% solution in plant oil, kindly provided by D. Shafritz). Blood plasma was isolated 30 hours post injection and at the time of sacrifice. ALT levels were determined by the Chemistry Laboratory of the Jacobi Medical Center.

FACS analysis of hematopoietic cells

Fetal livers were dissected from staged embryos and dissociated by gently pressuring them through a 40 μm cell strainer. Cell suspensions were stained in 4% FBS/PBS with biotinylated antibodies against the lineage markers B220 (RA3-6B2, Pharmingen, San Diego, CA), CD3 (145-2C11), CD4 (L3T4), CD19 (1D3), Gr1 (RB6-8C5) and Ter119 (TER-119) and the stem cell markers Sca1 (D7, PE-conjugated), and Kit (2B8, APC-conjugated) followed by Alexa Fluor 680®-conjugated streptavidin (Molecular Probes, Eugene, OR). Adult bone marrow cells were harvested from hind limb bones and mature erythrocytes lysed as described (Ye et al., 2003). For the analysis of adult HSCs antibodies against Mac1 (M1/70) and CD34 (RAM34) were included in the lineage mix. Dead cells were excluded by either DAPI (0.4 μg/ml) or propidium iodide (1 μg/ml) staining. Analyses were performed with either an LSRII flow cytometer (Becton-Dickinson) or a cell sorter (MoFlo-MLS, Cytomation, Fort Collins), collecting 1,000,000-2,500,000 events per sample. Data analysis was done with FlowJo (San Carlos, CA) software.

Preparation of frozen tissue sections

Mice were anesthetized and slowly perfused with 10 ml ice-cold PBS followed by 15 ml 4% paraformaldehyde (PFA) using a 23 gauge butterfly needle inserted into the left ventricle. The organs of interest were dissected out and fixed in 15 ml 1.5% PFA in 30% sucrose/PBS for 1 hour at 4°C after which they were sliced into 1-2 mm thick blocks and incubated for another 8-12 hours in the fixation solution. The blocks were washed twice with 30% sucrose/PBS, dried with tissue paper, embedded in OCT compound (Sakura, Torrance, CA) and submersed in 2-methylbutane at –80°C. Sections (10 μm) were cut using a cryostat (Leica CM1900), transferred onto pre-cleaned glass slides (Superfrost/Plus, Fisher Scientific) and stored at –80°C.

Analysis of frozen sections

Immunofluorescence was performed using the M.O.M. basic kit (Vector Labs, Burlingame, CA) following the manufacturer's instructions with the additional inclusion of 0.3% Triton-100 in all solutions and of 3% BSA and 5% goat serum in the blocking solution. For hepatocyte analysis, liver sections were stained with a cocktail of APC-conjugated antibodies against the hematopoietic markers CD45 (Pharmingen, 30-F11), F4/80 (Caltag, Burlingame, CA) and Mac1. DAPI (0.4 μg/ml) was included to visualize nuclei. Sections were screened for YFP^+ hepatocytes using a Nikon Eclipse E600 microscope equipped with a 40× objective and filters to visualize DAPI (Chroma #31000), YFP (Chroma #41028), Alexa Fluor® 546 (Chroma #41002c) and APC (Chroma #41013). Images were taken using a MagnaFire (Optronics, Goleta, CA) camera and analyzed with Adobe Photoshop software. Hepatocytes were identified based on cell morphology (brightfield), morphology of the nucleus (DAPI filter), absence of hematopoietic markers (APC filter) and their characteristic cytoplasmic autofluorescence (red filter). Slides containing YFP^+

hepatocytes were stained with an antibody against mouse albumin (Accurate, Westbury, NY) followed by an Alexa Fluor 546-conjugated secondary goat anti-rabbit antibody (Molecular Probes). The number of hepatocytes in a section was calculated as follows. First, the total area of the section was determined using low magnification images (2× objective) and Adobe Photoshop. This area value was multiplied with the average number of hepatocytes per high magnification field (40× objective, n=20 images) and with 400 (the difference in area magnification between a 2× and a 40× objective). Finally, the total number of hepatocytes was adjusted by multiplication with a 'fluorescence factor' between 0.7 and 0.9, as most sections contained small areas in which YFP fluorescence was not preserved.

For endothelial cell analysis, frozen sections were first stained with an antibody against CD45 (30-F11) followed by an Alexa Fluor 546-conjugated secondary goat anti-mouse antibody (Molecular Probes) and DAPI. After washing, the sections were stained with an APC-conjugated antibody against CD31 (MEC13.3). Images were taken as described above.

Analysis of endothelial cells by FACS

For the analysis of liver and kidney endothelial cells, mice were perfused into the left ventricle using the solutions described previously for rat liver perfusion (Neufeld, 1997) but replacing collagenase with Liberase Blendzyme 3 (0.21 U/ml, Roche Diagnostics, Indianapolis, IN). The dissected organs were incubated with the enzyme at 37°C for 45 minutes under gentle rotation. Cells were then dissociated with a 25 ml pipette, filtered through a 40 μm cell strainer, large cells removed by centrifugation at 30 ***g*** for 1 minute and the supernatant centrifuged at 300 ***g*** for 5 minutes. The pellet was washed twice with 4% FBS/PBS and then resuspended in the same solution. For FACS analysis, the cells were incubated for 5 minutes with anti-mouse CD16/32 antibody (FcBlock, Pharmingen) to block unspecific binding and then stained with antibodies against CD45, Ter119 (both PE-conjugated) and CD31 (APC-conjugated). FACS analyses were performed as described for hematopoietic cells. Staining with DAPI showed the viability of the isolated endothelial cells to be between 50%-85%.

Results

A mouse model that allows tracing hematopoietic cell ancestry throughout development

To determine whether hematopoietic cells contribute to non-hematopoietic cell types, we developed a transgenic mouse line expressing Cre recombinase from promoter/enhancer elements of the pan-hematopoietic *vav* gene (Fig. 1A). These regulatory elements have been shown to be active in all hematopoietic lineages, as well as in fetal hematopoietic progenitors (Ogilvy et al., 1999) and adult HSCs (Almarza et al., 2004) but are inactive in non-hematopoietic cells (de Boer et al., 2003; Ogilvy et al., 1999). The vav-Cre construct also contained an IRES-YFP cassette to visualize Cre-expressing cells but this element was found to be completely inactive in vivo (data not shown). Of five transgenic founders obtained, one was crossed with the ROSA26R-lacZ and the ROSA26R-YFP reporter lines, in which Cre mediated excision of a stop cassette leads to the irreversible activation of reporter gene expression in the Cre expressing cell and all its progeny (Soriano, 1999; Srinivas et al., 2001) (Fig. 1A). Analysis of vav-Cre/ROSA26R double-transgenic mice revealed segregation into two distinct phenotypes. About 70% of the mice showed reporter gene expression in essentially all nucleated blood cells but little outside of the hematopoietic system and were called 'vav ancestry mice'. The remaining 30% of the animals also exhibited pan-hematopoietic labeling but in addition expressed the reporter gene in 20-80% of all non-hematopoietic cell types. Animals with this wide expression pattern, called 'chimeric control mice', were used as positive controls. The latter phenotype can be explained by a transient and stochastic expression of the vav-Cre transgene in early blastomeres, a phenomenon also observed with lck-Cre transgenic mice (Ye et al., 2003). Examining ear clips revealed reporter positive, non-hematopoietic skin cells only in chimeric control mice, thus serving as a simple method to distinguish them from vav ancestry mice. The breeding scheme for these mice is shown in Fig. 1B.

Vav ancestry mice show an essentially complete labeling of their fetal and adult HSC populations

To determine the degree of hematopoietic labeling in vav ancestry mice, peripheral blood, bone marrow and spleen cells were analyzed by flow cytometry. As expected, >99% of nucleated bone marrow cells (lymphocytes, myeloid cells and erythroid precursors) as well as platelets were YFP positive (Fig. 1C; data not shown). To investigate whether HSCs are also labeled, we analyzed lineage$^-$Sca1$^+$c-kit$^+$ (LSK) cells from adult bone marrow and E13.5 fetal liver. This population, which contains all long-term repopulating stem cells (Christensen and Weissman, 2001; Morrison et al., 1995; Sanchez et al., 1996), exhibited a YFP labeling index of 99-100% in adult bone marrow and 93-96% in fetal liver (Fig. 1C,D). Earlier stages of development were assessed by the analysis of frozen sections, showing that ~50% of CD45$^+$ cells in E10.5 (36 somite pairs) fetal liver were reporter positive. These cells probably represent myeloid progenitors of yolk sac origin (Godin and Cumano, 2002). In addition, a small percentage of YFP$^+$ cells were found in the embryonic circulation at E9.5 (22 somite pairs), most of which corresponded to nucleated cells expressing the erythroid marker Ter119. These results show that essentially all definitive blood cells and a significant proportion of yolk sac-derived primitive blood cells are YFP labeled in vav ancestry mice.

Lysozyme ancestry mice are a complementary tool for hematopoietic lineage tracing

Because in vav ancestry mice all HSCs, committed progenitors and other nucleated hematopoietic cells are YFP labeled, this model alone does not allow drawing conclusions about the identity of the responsible cell type, in case evidence for hematopoietic plasticity are found. Therefore, LysM-Cre mice (Clausen et al., 1999) were bred with ROSA26 reporter mice containing either YFP or *lacZ*. In the resulting lysozyme ancestry mice, Cre expression from the endogenous lysozyme M locus leads to the irreversible activation of ROSA26 driven YFP in about ~90% of blood myelomonocytic cells (Ye et al., 2003) and essentially 100% of tissue macrophages (data not shown). In addition, a varying subset of adult long-term reconstituting HSCs and of all other hematopoietic cell types is reporter positive as a consequence of myeloid linage priming in HSCs (Ye et al., 2003). The degree of labeling of the LSK population ranges from ~3% to ~30%, depending on the animal, and can be reliably deduced from the labeling index of peripheral B cells (Ye et al., 2003). As macrophages are therefore the only cell

type completely labeled in both ancestry models (Fig. 1E), contributions of these cells to non-hematopoietic cells should lead to the same labeling frequencies in both mouse models, while contributions involving another hematopoietic cell type should be found less frequently in lysozyme than in vav ancestry mice.

Concomitant identification of reporter positive hepatocytes, endothelial cells and hematopoietic cells in chimeric control mice

Chimeric control mice, expressing either YFP or *lacZ*, were used to determine optimal conditions of tissue-preparation for reporter gene detection in frozen sections. We found that

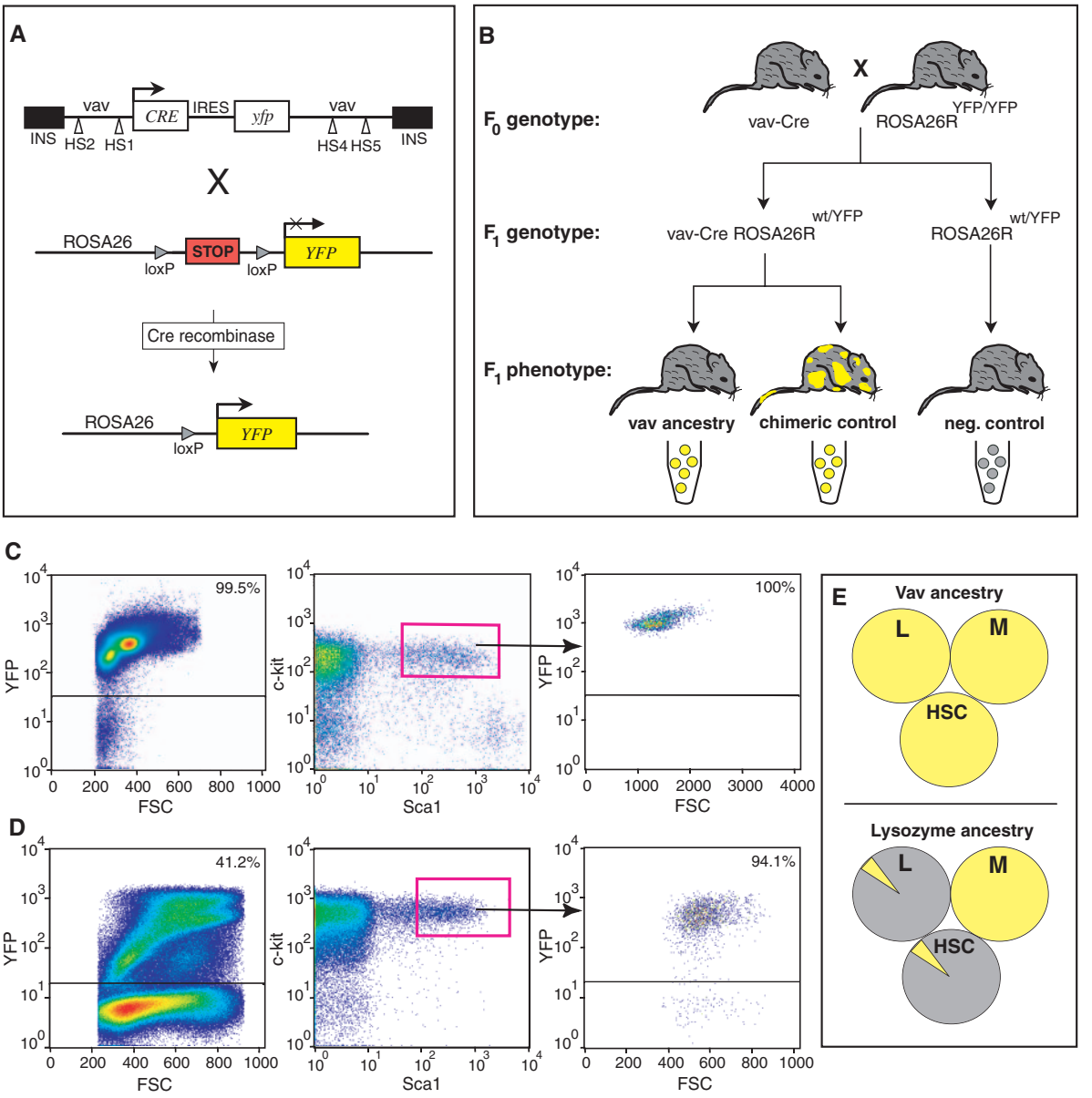

Fig. 1. Generation and hematopoietic labeling of the ancestry mice. (A) Structure of the vav-Cre transgenic vector showing the hypersensitivity sites (HS) of the vav elements, the insulator sequences (INS) and the IRES-YFP element, which was not functional in vivo (indicated by the lowercase letters), and of the ROSA26R-YFP locus before and after Cre-mediated excision of the stop cassette. (B) Cross of vav-Cre transgenic mice with ROSA26R-YFP mice. F1 animals with the vav-Cre transgene segregated into two phenotypes, which were distinguished by the expression of YFP in the skin of chimeric control mice (yellow patches) and the absence of such a labeling in vav ancestry mice. The F1 mice without the vav-Cre transgene were used as negative controls. The tubes at the bottom containing grey or yellow 'cells' indicate the degree of hematopoietic labeling in the different mice. (C) FACS analysis of mononucleated cells from adult bone marrow for YFP expression (left plot). LSK cells were gated (box, middle plot) and analyzed for YFP expression (right plot). (D) FACS analysis of whole E13.5 fetal liver (left plot). LSK cells were gated (box, middle plot) and analyzed for YFP expression (right plot). Numbers in the top right-hand corner of the plots indicate the percentage of YFP^+ cells in the respective cell population. FSC, forward scatter. (E) Comparison of the hematopoietic labeling of vav ancestry and lysozyme ancestry mice. The circles represent cell compartments: L, lymphoid; M, myelomonocytic and HSC, hematopoietic stem cells. Yellow indicates that the cells in a given compartment are YFP labeled, grey that they are unlabeled. The yellow triangles indicate that a subset of cells in the corresponding compartment is YFP^+.

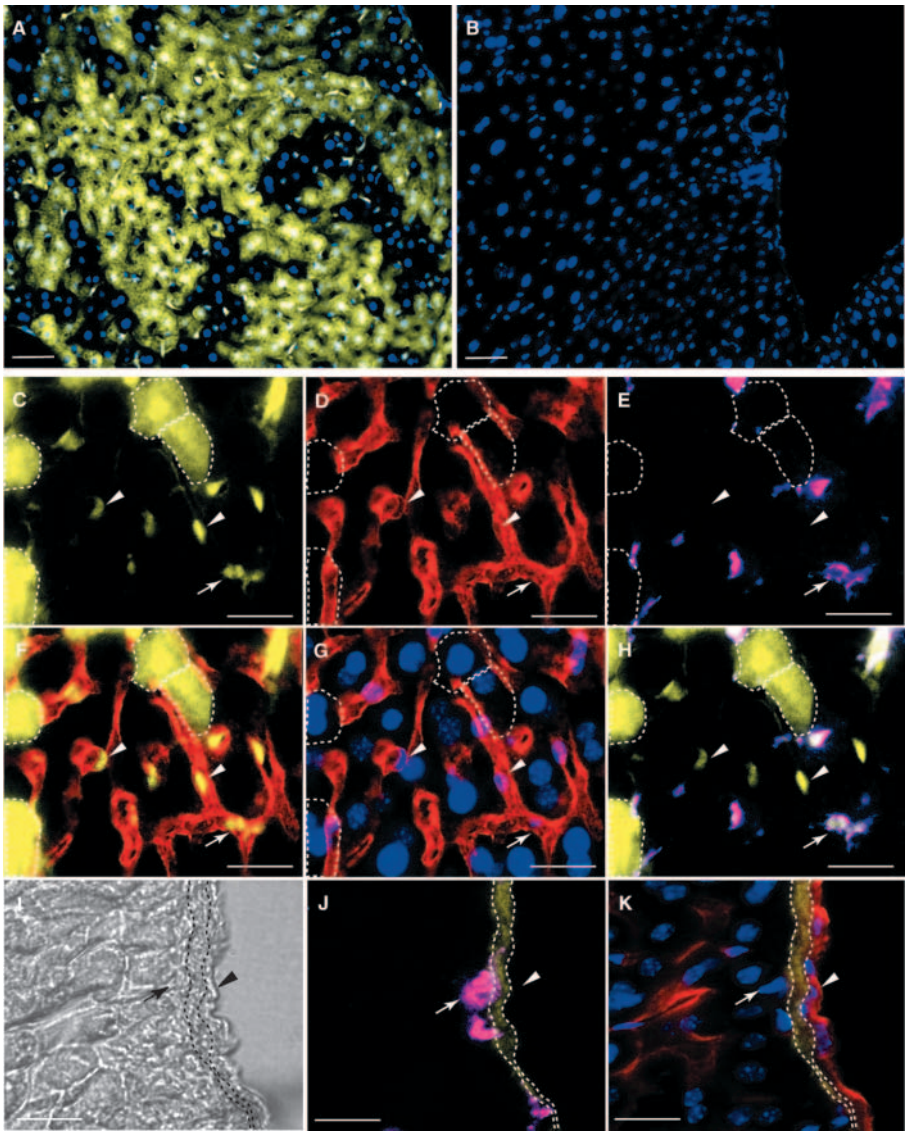

Fig. 2. Identification of hepatocytes and endothelial cells in control mice. (A,B) Liver sections from a chimeric control (A) and a negative control mouse (B) showing DAPI stained nuclei (blue) and YFP fluorescence (yellow). Scale bar: 50 µm. (C-H) Frozen liver section from a chimeric control mouse showing hepatic sinusoids: YFP (yellow); CD31 (red); CD45 (purple); DAPI (blue). YFP$^+$ hepatocytes are outlined with a broken line, arrowheads highlight two representative YFP+ endothelial cells; arrow shows the position of one hematopoietic cell close to a vessel. Scale bar: 25 µm. (I-K) Frozen liver sections from a negative control mouse showing part of a larger hepatic vessel: autofluorescence (yellow); CD31 (red); CD45 (purple); DAPI (blue). The position of the autofluorescent basement membrane is indicated by broken lines. Arrows and arrowheads in I-K indicate the positions of hematopoietic cells and the endothelial cell layer, respectively. Scale bar: 25 µm.

direct YFP fluorescence yields the best signal-to-noise ratio and no false-positive cells. In addition, it is most conveniently combined with antibody staining to determine the identity of reporter gene expressing cells (Fig. 2A,B; data not shown). Hepatocytes were identified as large polygonal CD45$^-$ cells with prominent round nuclei. As shown in Fig. 2C-H, YFP$^+$ hepatocytes (broken white outline) could be clearly distinguished from adjacent YFP$^-$ hepatocytes in liver sections from chimeric control mice. Fig. 2C-H also shows that YFP$^+$ endothelial cells (white arrowheads) can be distinguished from YFP$^+$ hematopoietic cells (white arrows) by their strong expression of CD31 and absence of CD45. In general, YFP$^+$ cells showed strong nuclear fluorescence (compare Fig. 2F,G). This feature facilitated the distinction between YFP fluorescence and autofluorescence, which is largely cytoplasmic, especially in hepatocytes. As negative controls, we analyzed ROSA26R-YFP (that lack the vav-Cre transgene) and vav-Cre transgenic mice (that lack the floxed ROSA-YFP allele). Liver sections encompassing more than 500,000 hepatocytes from these mice revealed no evidence for spontaneous read-through of the stop cassette or re-activation of the IRES-YFP element. Larger hepatic vessels, such as portal veins, frequently exhibited a rim of extracellular autofluorescence that was strongest in the blue/green part of the spectrum. This rim, which was also seen in wild-type mice, most probably delineates the position of the basement membrane as endothelial cells were found on its luminal side and tissue hematopoietic cells on its abluminal side (Fig. 2I-K). Together, these pilot experiments show that YFP-positive hepatocytes, endothelial and hematopoietic cells can be readily identified by the lineage tracing approach taken.

Vav ancestry mice contain YFP$^+$ hepatocytes

To address the issue of whether hematopoietic cells function as hepatocyte precursors during development, we analyzed liver sections from vav ancestry mice. This revealed the presence of rare YFP$^+$ cells with hepatocyte morphology that did not express the hematopoietic markers CD45, Mac1 and F4/80 (Fig. 3A,B) and were randomly distributed within the liver parenchyma. As shown in Fig. 3C, the majority of the YFP$^+$ hepatocytes were single cells, with some being contained in clusters of two or three cells (in the following, all YFP$^+$ hepatocytes are referred to as ‘clusters’ even if they correspond to a single cell). These cluster sizes are slight under-representations as cells outside the plane of the 10 µm sections analyzed would have been missed. The YFP$^+$ hepatocytes are probably functional as they express albumin (Fig. 3D-F). The low frequency of YFP$^+$ hepatocyte clusters observed (1 in 79,000 hepatocytes, Table 1) was not due to poor reporter gene preservation, because essentially all hematopoietic cells in the sections scored were YFP positive. These findings provide evidence that hematopoietic

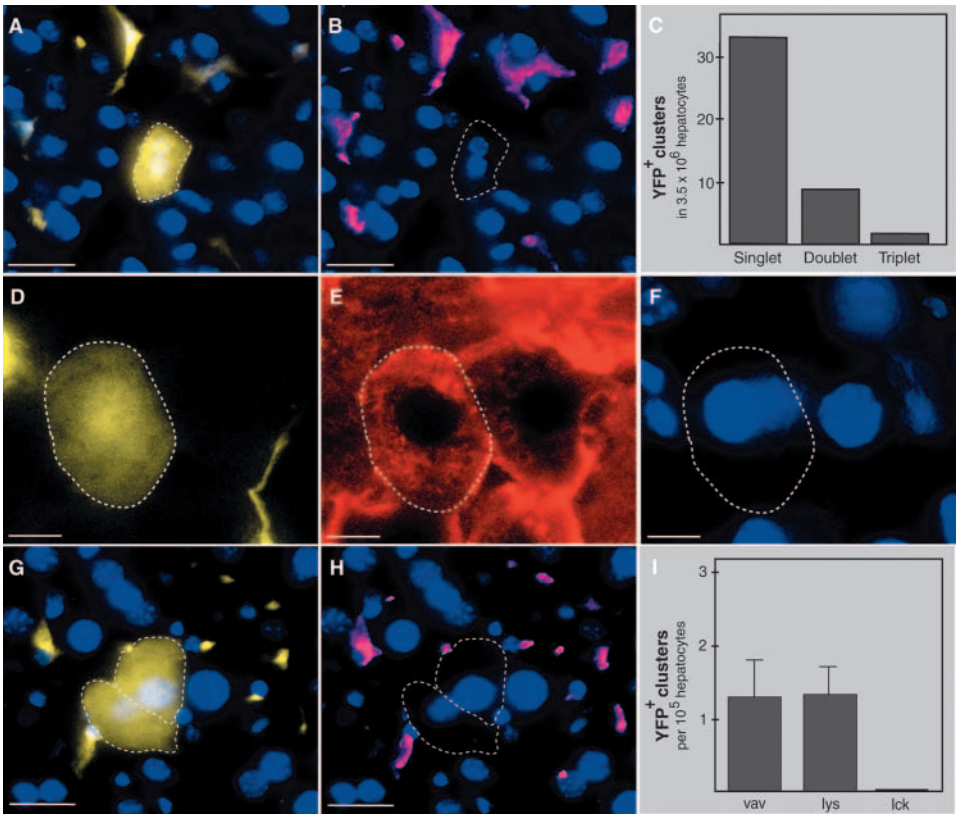

Fig. 3. Hepatocyte labeling in vav ancestry and lysozyme ancestry mice. (A,B) A binucleated YFP$^+$ hepatocyte (yellow, outlined) in a liver section of a vav ancestry mouse. Nuclei are stained with DAPI (blue) and hematopoietic cells with F4/80, Mac1 and CD45 (purple). Scale bar: 25 μm. (C) The total number and distribution of hepatocyte clusters in vav ancestry mice. (D-F) Liver section of a vav ancestry mouse showing an YFP$^+$ hepatocyte (yellow, outlined) that was stained for albumin expression (red). Nuclei are shown in blue. Scale bar: 10 μm. (G,H) Liver section of a lysozyme ancestry mouse showing a doublet of YFP$^+$ hepatocytes (yellow, outlined). Nuclei are shown in blue; Kupffer cells, stained with F4/80, are in purple. Scale bar: 25 μm. (I) The frequency of YFP$^+$ hepatocyte clusters per 100,000 cells in vav ancestry (vav), lysozyme ancestry (lys) and lck ancestry (lck) mice. Error bars indicate one s.d.

contributions to hepatocytes occur at a low frequency during normal development and that the resulting cells can divide.

Lysozyme ancestry mice contain similar numbers of YFP$^+$ hepatocytes as vav ancestry mice

In an attempt to determine the cell type involved in the observed contributions, liver sections from one lysozyme ancestry mouse with a high (26%) and two with a low degree (3% and 4%) of LSK labeling were analyzed. In a total of more than 1 million hepatocytes scored, we found 20 YFP$^+$ cells (Fig. 3G-H; Table 1). These cells also expressed albumin and were distributed among 12 singlets and four doublets. Although the total number of YFP$^+$ hepatocytes detected was low, their frequency did not differ significantly in mice with high and low HSC labeling (Table 1). In addition, their average incidence (one in 73,000 hepatocytes) was similar to that found in vav ancestry mice (Fig. 3I). To rule out the possibility that other hematopoietic cells present in the liver contribute to hepatocyte formation, lck ancestry mice were analyzed. These mice are characterized by YFP expression in >95% of T lymphoid but no other hematopoietic cells. We found no YFP+ hepatocytes among 750,000 hepatocytes in liver sections from two such animals (Fig. 3l). Together, these results support the notion that hematopoietic contributions to hepatocytes involve macrophages in unperturbed mice.

Liver damage leads to a moderate increase of hepatocyte labeling in vav ancestry mice

To address the issue of whether liver injury increases the frequency of hematopoietic contributions to hepatocytes, two adult vav ancestry mice were injected with carbon tetrachloride (CCl_4) at a concentration that induces necrosis in ~60% of hepatocytes (Yuan et al., 2003). Thirty hours after injection, we measured the blood plasma levels of alanine amino transferase (ALT), an indicator for injury to the liver parenchyma. These

Table 1. Hepatocyte analysis in frozen sections

		Animal			
		1	2	3	4
Vav ancestry mice	Number of hepatocytes screened	1.05×10^6	0.98×10^6	0.84×10^6	0.63×10^6
	Number of YFP$^+$ clusters	12	14	6	12
	Frequency of YFP$^+$ clusters	1:87,500	1:70,000	1:140,000	1:52,500
Lysozyme ancestry mice	Number of hepatocytes screened	0.47×10^6	0.41×10^6	0.29×10^6	–
	Number of YFP$^+$ clusters	8	4	4	–
	Frequency of YFP$^+$ clusters	1:58,800	1:102,500	1:72,500	
	% labeling of LSK cells	26	4	3	–
Vav ancestry mice (+CCl_4)	Number of hepatocytes screened	0.47×10^6	0.53×10^6	–	–
	Number of YFP$^+$ clusters	18	16	–	–
	Frequency of YFP$^+$ clusters	1:25,800	1:33,100	–	–

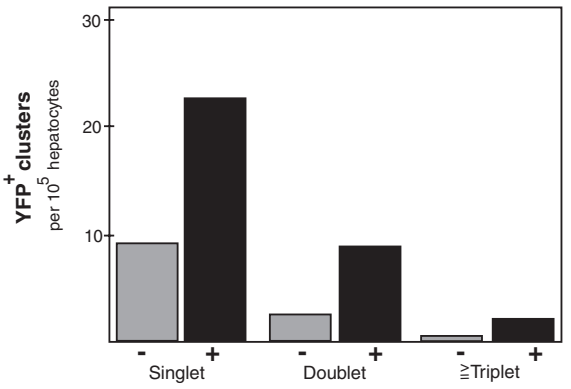

Fig. 4. Effect of liver injury on hematopoietic to hepatocyte contributions. Distribution of YFP labeled hepatocyte clusters of injured (black bars) and uninjured (gray bars) vav ancestry mice. A total of 995,000 hepatocytes from two vav ancestry mice 3 weeks after CCl_4 injection were analyzed. The values for uninjured vav ancestry are the same as in Fig. 3C. Clusters containing three or more YFP^+ hepatocytes (the latter were only found in injured mice) were pooled in one group.

were determined to be 26 units per liter (U/I) for a control vav ancestry mouse injected with oil and 4660 U/I and 7740 U/I for the injured mice. The experimental mice were sacrificed 3 weeks after CCl_4 administration, at which time they exhibited plasma ALT levels of 31 U/I and 18 U/I, respectively. Compared with uninjured mice, liver sections of the injured mice revealed a two- to threefold increase in the frequency of YFP^+ hepatocyte clusters (~1 in 26,000 and ~1 in 33,000, respectively, Table 1) and a slight increase in cluster size, with clusters containing up to five YFP^+ hepatocytes (in the plane of a 10 μm section). The cluster size distribution compared with uninjured mice is shown in Fig. 4.

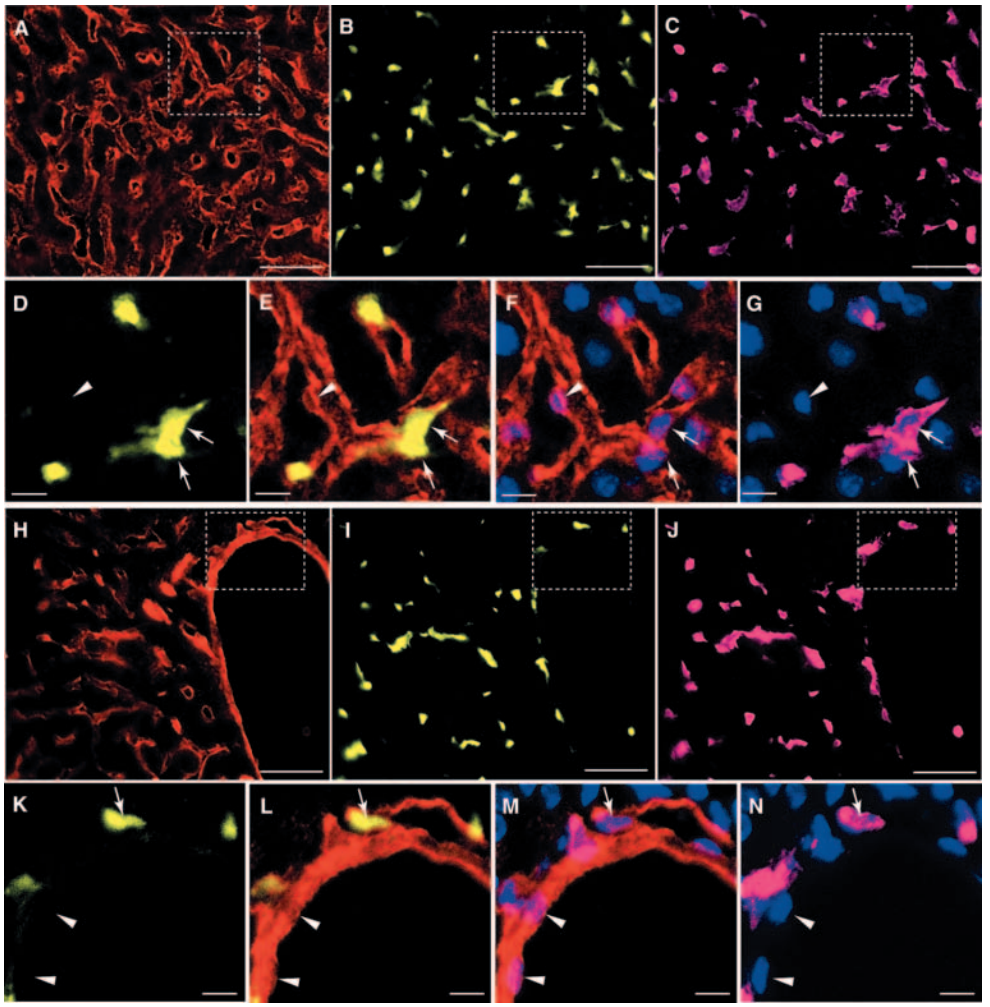

Fig. 5. Analysis of hepatic endothelial cells in vav ancestry mice. (A-C) Frozen section showing sinusoidal endothelial cells (CD31, red), YFP fluorescence (yellow) and hematopoietic cells (CD45, purple). Scale bar: 25 μm. (D-G) Magnification of the area boxed in A-C, showing an YFP^- endothelial cell (arrowhead) and two YFP^+ hematopoietic cells (arrows) that are closely associated with the sinusoids. DAPI (blue), CD31 (red), YFP (yellow) and CD45 (purple). Scale bar: 10 μm. (H-J) Area with a large hepatic vessel visualized by CD31 staining (red). YFP (yellow), CD45 (purple). Hematopoietic cells closely line the vessel. Scale bar: 25 μm. (K-N) Magnification of the area boxed in H-J showing two YFP^- endothelial cells (arrowheads) integrated into the vessel wall and one YFP^+ hematopoietic cell on the abluminal side of the endothelial lining: DAPI (blue); CD31 (red); CD45 (purple). Scale bar: 10 μm.

Absence of YFP^+ hepatic endothelial cells in vav ancestry mice

To determine whether hematopoietic cells contribute to endothelial cells during mouse development, we analyzed 20-30 liver sections from three adult vav ancestry mice. Large numbers of YFP^+ cells were found in close association with the sinusoidal microvasculature of the liver. However, all of these cells were hematopoietic, as shown by the expression of CD45 (Fig. 5A-C) and most of them corresponded to Kupffer cells as they also expressed F4/80. Sinusoidal endothelial cells were uniformly YFP^- (Fig. 5D-G). An analogous situation was found in larger hepatic vessels, such as portal veins, where YFP^+ hematopoietic cells lined the basement membrane on its abluminal side (Fig. 5H-J). Most of these cells expressed low levels or no F4/80 but were Mac1 and/or CD11c positive (indicative of macrophages and myeloid dendritic cells), while others expressed CD3 (indicative of T cells). No

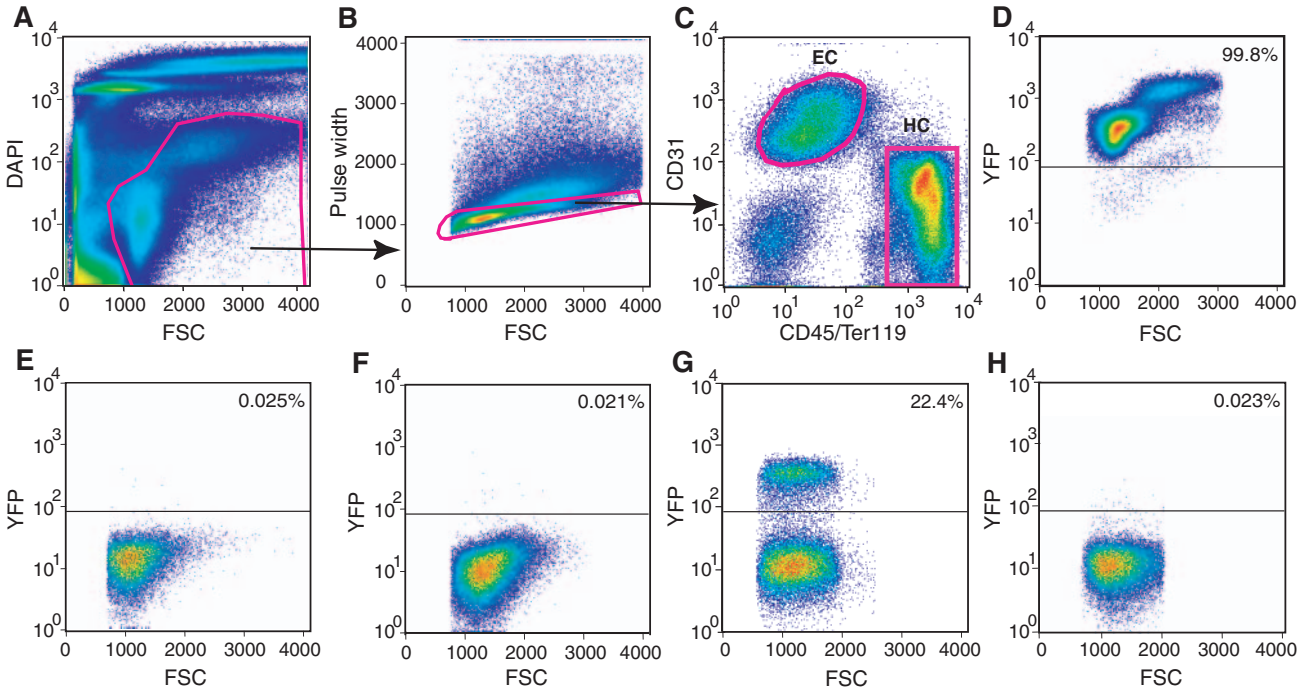

Fig. 6. FACS analysis of liver cell suspensions. (A-C) Gating logic for cells in organ cell suspension based on exclusion of dead cells by DAPI staining (A) and doublets by pulse width analysis (B). (C) Endothelial cells (EC) and hematopoietic cells (HC) are defined by marker gene expression. (D) YFP labeling of CD45+ hematopoietic cells isolated from the liver of a vav ancestry mouse. (E-H) YFP labeling of hepatic endothelial cells from a negative control mouse (E), a vav ancestry mouse (F), a chimeric control mouse (G) and a wild-type mouse completely reconstituted (>95%) with bone marrow of a vav ancestry mouse three months after transplantation (H).

Table 2. FACS analysis of endothelial cells

		Vav ancestry mice			Negative control mice	
		1	2	3	1	2
Liver	Number of cells analyzed	3.0×10^4	5.8×10^4	5.3×10^4	1.0×10^4	3.3×10^4
	Number of YFP$^+$ cells	7	14	11	2	8
	% YFP$^+$ cells	0.023	0.024	0.021	0.020	0.024
Kidney	Number of cells analyzed	15.3×10^4	8.7×10^4	7.8×10^4	1.9×10^4	–
	Number of YFP$^+$ cells	284	123	87	5	–
	% YFP$^+$ cells	0.19	0.14	0.11	0.021	–

endothelial cells in larger vessels were found to express YFP (Fig. 5K-N).

To strengthen these observations, liver cell suspensions were analyzed by flow cytometry. Dead cells were excluded by DAPI staining and aggregates by pulse width analysis. Hematopoietic and endothelial cells were distinguished by the expression of cell surface antigens (the gating logic is illustrated in Fig. 6A-C). As expected, >99% of CD45$^+$ hematopoietic cells in vav ancestry mice were also YFP$^+$ (Fig. 6D). By contrast, no YFP$^+$ cells above background levels were found in >140,000 endothelial cells from three different vav ancestry mice (Fig. 6E,F and Table 2), while YFP$^+$ hepatic endothelial cells from chimeric control mice formed a distinct population (Fig. 6G). This indicates that hepatic endothelial cells do not originate from hematopoietic cells during development. Furthermore, we found no evidence for endothelial cells of hematopoietic origin 3 months after the transplantation of bone marrow from a vav ancestry mouse into a lethally irradiated non-transgenic littermate (Fig. 6H, ~40,000 endothelial cells were analyzed).

To determine whether similar observations as in the liver can be made in another highly vascularized organ, endothelial cells from the kidney were also subjected to FACS analysis. As shown in Fig. 7 and Table 2, kidney cell suspensions from vav ancestry mice contained 0.11% to 0.19% YFP$^+$ endothelial cells. The analysis of frozen kidney sections from three vav ancestry mice revealed that 20-40% of the endothelial cells in vasa recta, capillaries carrying blood in and out of the kidney medulla, expressed YFP. As no other endothelial cells were found to be YFP$^+$ in kidney sections, vasa recta cells probably correspond to the labeled cells found by flow cytometry. However, no such cells could be detected in mice fully re-constituted with bone marrow from vav ancestry (Fig. 7D). Furthermore, kidney sections from two lysozyme ancestry mice, one with 3% and one with 30% LSK labeling, revealed no YFP$^+$ endothelial cell in >30 vasa recta bundles scored for each mouse (data not shown). These observations argue against a hematopoietic origin of vasa recta endothelial cells.

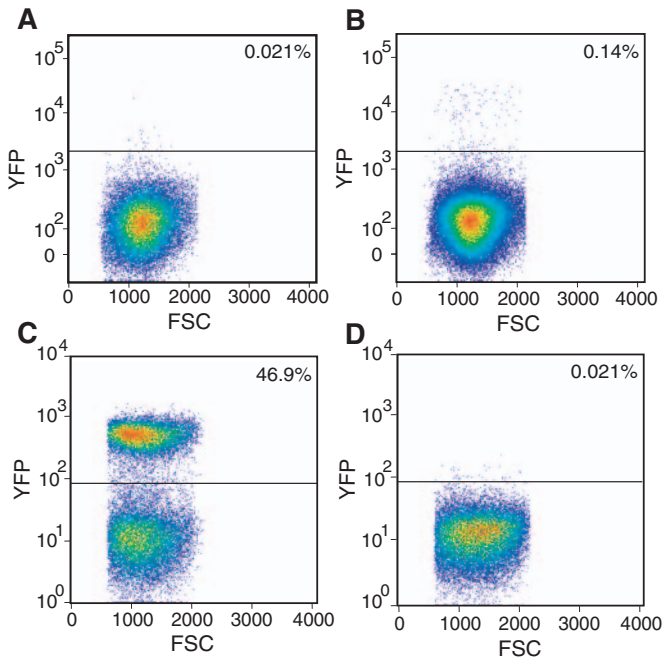

Fig. 7. Analysis of renal endothelial cells by flow cytometry. (A-D) YFP labeling of endothelial cells in kidney cell suspensions from a negative control mouse (A), a vav ancestry mouse (B), a chimeric control mouse (C) and a wild-type mouse completely reconstituted with bone marrow of a vav ancestry mouse three months after transplantation (D). The YFP$^+$ cells in B correspond to vasa recta endothelial cells. The data shown in A,B were obtained using the MoFlo cell sorter and the LSRII flow cytometer, respectively; hence, the different representation of the YFP intensity.

Discussion

Hematopoietic cells contribute to hepatocytes in unperturbed animals

The similar frequency of YFP$^+$ hepatocytes observed in vav and lysozyme ancestry mice indicates a hematopoietic origin of these cells. However, formally the possibility still exists that the vav-Cre transgene and the lysozyme Cre knock-in are co-expressed in a small subset of hepatocytes. Several reasons argue against this possibility. First, the vav elements used have been shown to be inactive in hepatocytes (Ogilvy et al., 1999). Second, the activities of vav-Cre and lysozyme-Cre in non-hematopoietic cell types such as precursors of cardiac, neuronal and skeletal muscle cells show no overlap (M.S. and T.G., unpublished). Finally, the absence of YFP$^+$ hepatocytes in the lck ancestry mouse demonstrates that another hematopoietic specific transgene yielding a 'chimeric control' phenotype is absolutely silent in hepatocytes. Taken together, this strongly suggests that hematopoietic to hepatocyte conversions do occur in normal mice and do not depend on transplantation, induction of liver injury or the genetic abnormalities of the FAH model.

Hematopoietic to hepatocyte contributions do not occur during early stages of development

The vast majority of LSK cells from E13.5 fetal liver of vav ancestry mice already express YFP at maximum levels (Fig. 1D). This implies that vav-Cre expression begins shortly after the emergence of the first HSCs, as there is an inherent delay between Cre expression and reporter gene activation (Prost et al., 2001). The presence of YFP$^+$ hematopoietic cells in E10.5 fetal liver shows that yolk sac-derived progenitors, which home to the fetal liver before the colonization of this organ by HSCs, are also labeled in vav ancestry mice. Together, these observations suggest that even the earliest hematopoietic to hepatocyte contributions should have been detected in the vav ancestry model. The number of hepatocytes increases ~100 fold between E13.5 and adulthood (Anzai et al., 2003; Wang et al., 2002), resulting in a liver that is a mosaic of clonally derived colonies (Kennedy et al., 1995; Shiojiri et al., 2000), as can also be seen in chimeric control mice (Fig. 2A). Therefore, early hematopoietic contributions should have led to clusters of 100 or more YFP$^+$ hepatocytes in adult vav ancestry mice. The absence of such clusters therefore strongly argues against fetal hematopoietic to hepatocyte contributions. This implies that the mouse fetal liver environment, which supports the proliferation and differentiation of hepatocytes and their precursors, does not trigger a hepatic potential in hematopoietic cells. In addition, the observed prevalence of single YFP$^+$ hepatocytes suggests that few, if any, conversions occur perinatally, as the liver weight increases 20-fold after birth (Lau et al., 2003). We therefore conclude that hematopoietic plasticity plays no role in liver development.

Macrophages are the source for the observed hematopoietic contributions to hepatocytes

A possible explanation for the absence of hematopoietic contributions in the embryo is that the fetal liver lacks the cell types involved in the process. Thus, there could be a requirement for mature hepatocytes, cells whose differentiation is completed only around birth (Zaret, 2002). Alternatively, the relevant blood cell type might be the Kupffer cell, a specialized tissue macrophage that develops postnatally (Morris et al., 1991). This possibility is supported by the observation that vav and lysozyme ancestry mice exhibit similar frequencies of labeled hepatocytes. Any significant contribution of hematopoietic cells other than macrophages should have led to a greater than 20-fold difference in the hepatocyte labeling index between vav ancestry mice and the two lysozyme ancestry mice with a low HSC labeling index studied (Table 1). It is also unlikely that YFP$^+$ HSCs of lysozyme ancestry mice are particularly plastic, as we found no significant differences in the hepatocyte labeling indices between mice with low and high HSC labeling (Table 1). Finally, the observations with the lck ancestry mouse rule out a contribution of T lineage cells. The conclusion that macrophages contribute to hepatocytes during normal development is in agreement with observations made after transplantation of hematopoietic cells into FAH-deficient mice (Camargo et al., 2004; Willenbring et al., 2004). In addition, the frequency of labeled hepatocyte clusters observed in our study, ~650 per liver, falls within the range of hematopoietic derived colonies in the FAH model (Camargo et al., 2004; Wang et al., 2002; Willenbring et al., 2004), suggesting that hepatic contributions occurring during normal development are also mediated by cellular fusion.

The two- to threefold elevated number of YFP$^+$ hepatocyte clusters observed after CCl_4 injection might be best explained by an inflammatory response that leads to an increase in the

number of activated liver macrophages and consequently to additional fusions with hepatocytes. The increased cluster size in response to liver injury shows that hepatocytes of hematopoietic origin can divide normally.

Hematopoietic stem cells do not function as hemangioblasts during mouse development

The absence of YFP$^+$ endothelial cells in the liver strongly indicates that hematopoietic cells do not contribute to the formation of hepatic endothelial cells during development. Thus, although the first vascular structures develop at E9.5 in the liver primordium (Matsumoto et al., 2001), the majority of endothelial cells are generated during subsequent organ growth, at a time when most hematopoietic cells are already YFP labeled in vav ancestry mice. Further support for the conclusion that definitive HSCs, which originate from the endothelial cell layer of the dorsal aorta, have lost their endothelial potential comes from the lack of YFP$^+$ endothelial cells in the heart, brain and lung of vav ancestry mice (data not shown). The situation in the kidney is more complex as an endothelial subset contained in the vasa recta is YFP labeled. Because no such cells were found in lysozyme ancestry mice or after the transplantation of vav ancestry bone marrow, we do not believe that they are of hematopoietic origin. However, we cannot entirely rule out a contribution made by hematopoietic cells exclusively labeled in the vav ancestry model and not present in adult bone marrow.

Our inability to detect hematopoietic to endothelial cell conversions was unexpected based on reports describing such transitions after transplantation of HSCs either with or without additional injury (Bailey et al., 2004; Grant et al., 2002; Sata et al., 2002; Tamura et al., 2002). This apparent discrepancy cannot simply be due to transplantation-associated injuries as we could not detect YFP$^+$ endothelial cells in mice reconstituted with bone marrow cells from vav ancestry mice (Fig. 6H; Fig. 7D). A possible explanation might be differences in the criteria used to identify endothelial cells. For example, in one study (Bailey et al., 2004), endothelial cells were identified as expressing lower levels of CD31 than hematopoietic cells, whereas we found the opposite to be the case (Fig. 6C). In addition, in studies where sections were not simultaneously stained for the expression of hematopoietic and endothelial markers (Gao et al., 2001; Grant et al., 2002; Sata et al., 2002; Tamura et al., 2002), hematopoietic cells might have been erroneously identified as endothelial cells due to the close apposition of the two cell types (see, for example, Fig. 2C-H, Fig. 5). Finally, in reports using GFP as a reporter (Bailey et al., 2004), endothelial cells might have been misidentified as being of donor origin due to the autofluorescence of their basement membrane (Fig. 2J,K). In this regard chimeric control mice provided a unique tool to exclude artifacts and to optimize conditions for the identification of different types of reporter labeled cells. However, it is still possible that hematopoietic to endothelial cell conversions occur in organs not analyzed in this study or can be induced, for example when cells in the retina are injured and exposed to VEGF (Grant et al., 2002). Perhaps injury-mediated re-vascularization is fundamentally different from normal vasculogenesis and angiogenesis.

Another issue is the origin and function of endothelial progenitor cells, which have been observed in the embryo (Wei et al., 2004) and in the circulation after bone marrow transplantation (Asahara et al., 1999). Our data suggest that they are either not of hematopoietic origin or, if so, they are not involved in the generation of endothelial cells during normal ontogeny. Of note, CD45$^-$Mac1$^-$CD31$^-$ cultured bone marrow stromal cells of vav ancestry mice are YFP$^-$ (M.S. and T.G., unpublished). Whether these cells or other rare non-hematopoietic bone marrow subsets have angiogenic potential remains to be determined.

In summary, our data indicate that once HSCs are specified, neither they nor their progeny become reprogrammed into hepatocytes or endothelial cells during fetal or early postnatal development. Furthermore, while macrophage to hepatocyte contributions can be detected as an ongoing process in the adult mouse, they do not constitute a significant source of cell replacement during normal tissue maintenance or regeneration. Our work thus supports the classical concept that germ layer specification sets developmental boundaries.

We thank Jerry Adams for the vav promoter construct; Adam West for the insulator elements; Todd Evans, Kelly McNagny, Fabio Rossi, Cathy Laiosa, Huafeng Xie and Min Ye for comments on the manuscript; David Shafritz for suggestions and materials; David Neufeld for help with liver perfusions; and Kristie Gordon from the Albert Einstein Cancer Research center FACS facility for cell sorting. This work was supported by NIH grant RO1 NS43881-01 (T.G.) and by a scholarship from the Boehringer Ingelheim Fonds (M.S.).

References

Almarza, E., Segovia, J. C., Guenechea, G., Gomez, S. G., Ramirez, A. and Bueren, J. A. (2004). Regulatory elements of the vav gene drive transgene expression in hematopoietic stem cells from adult mice. *Exp. Hematol.* **32**, 360-364.

Almeida-Porada, G., Porada, C. D., Chamberlain, J., Torabi, A. and Zanjani, E. D. (2004). Formation of human hepatocytes by human hematopoietic stem cells in sheep. *Blood* **104**, 2582-2590.

Anzai, H., Kamiya, A., Shirato, H., Takeuchi, T. and Miyajima, A. (2003). Impaired differentiation of fetal hepatocytes in homozygous jumonji mice. *Mech. Dev.* **120**, 791-800.

Asahara, T., Masuda, H., Takahashi, T., Kalka, C., Pastore, C., Silver, M., Kearne, M., Magner, M. and Isner, J. M. (1999). Bone marrow origin of endothelial progenitor cells responsible for postnatal vasculogenesis in physiological and pathological neovascularization. *Circ. Res.* **85**, 221-228.

Bailey, A. S., Jiang, S., Afentoulis, M., Baumann, C. I., Schroeder, D. A., Olson, S. B., Wong, M. H. and Fleming, W. H. (2004). Transplanted adult hematopoietic stems cells differentiate into functional endothelial cells. *Blood* **103**, 13-19.

Blau, H. M., Brazelton, T. R. and Weimann, J. M. (2001). The evolving concept of a stem cell: entity or function? *Cell* **105**, 829-841.

Bloor, A. J., Sanchez, M. J., Green, A. R. and Gottgens, B. (2002). The role of the stem cell leukemia (SCL) gene in hematopoietic and endothelial lineage specification. *J. Hematother. Stem Cell Res.* **11**, 195-206.

Camargo, F. D., Finegold, M. and Goodell, M. A. (2004). Hematopoietic myelomonocytic cells are the major source of hepatocyte fusion partners. *J. Clin. Invest.* **113**, 1266-1270.

Choi, K., Kennedy, M., Kazarov, A., Papadimitriou, J. C. and Keller, G. (1998). A common precursor for hematopoietic and endothelial cells. *Development* **125**, 725-732.

Christensen, J. L. and Weissman, I. L. (2001). Flk-2 is a marker in hematopoietic stem cell differentiation: a simple method to isolate long-term stem cells. *Proc. Natl. Acad. Sci. USA* **98**, 14541-14546.

Clausen, B. E., Burkhardt, C., Reith, W., Renkawitz, R. and Forster, I. (1999). Conditional gene targeting in macrophages and granulocytes using LysMcre mice. *Transgenic Res.* **8**, 265-277.

de Boer, J., Williams, A., Skavdis, G., Harker, N., Coles, M., Tolaini, M., Norton, T., Williams, K., Roderick, K., Potocnik, A. J. et al. (2003). Transgenic mice with hematopoietic and lymphoid specific expression of Cre. *Eur. J. Immunol.* **33**, 314-325.

de Bruijn, M. F., Ma, X., Robin, C., Ottersbach, K., Sanchez, M. J. and Dzierzak, E. (2002). Hematopoietic stem cells localize to the endothelial cell layer in the midgestation mouse aorta. *Immunity* **16**, 673-683.
Ema, M., Faloon, P., Zhang, W. J., Hirashima, M., Reid, T., Stanford, W. L., Orkin, S., Choi, K. and Rossant, J. (2003). Combinatorial effects of Flk1 and Tal1 on vascular and hematopoietic development in the mouse. *Genes Dev.* **17**, 380-393.
Gao, Z., McAlister, V. C. and Williams, G. M. (2001). Repopulation of liver endothelium by bone-marrow-derived cells. *Lancet* **357**, 932-933.
Garcia-Castro, M. and Bronner-Fraser, M. (1999). Induction and differentiation of the neural crest. *Curr. Opin. Cell Biol.* **11**, 695-698.
Godin, I. and Cumano, A. (2002). The hare and the tortoise: an embryonic haematopoietic race. *Nat. Rev. Immunol.* **2**, 593-604.
Graf, T. (2002). Differentiation plasticity of hematopoietic cells. *Blood* **99**, 3089-3101.
Grant, M. B., May, W. S., Caballero, S., Brown, G. A., Guthrie, S. M., Mames, R. N., Byrne, B. J., Vaught, T., Spoerri, P. E., Peck, A. B. et al. (2002). Adult hematopoietic stem cells provide functional hemangioblast activity during retinal neovascularization. *Nat. Med.* **8**, 607-612.
Gurdon, J. B. and Byrne, J. A. (2003). The first half-century of nuclear transplantation. *Proc. Natl. Acad. Sci. USA* **100**, 8048-8052.
Herzog, E. L., Chai, L. and Krause, D. S. (2003). Plasticity of marrow-derived stem cells. *Blood* **102**, 3483-3493.
Hochedlinger, K. and Jaenisch, R. (2002). Monoclonal mice generated by nuclear transfer from mature B and T donor cells. *Nature* **415**, 1035-1038.
Jaffredo, T., Gautier, R., Eichmann, A. and Dieterlen-Lievre, F. (1998). Intraaortic hemopoietic cells are derived from endothelial cells during ontogeny. *Development* **125**, 4575-4583.
Jang, Y. Y., Collector, M. I., Baylin, S. B., Diehl, A. M. and Sharkis, S. J. (2004). Hematopoietic stem cells convert into liver cells within days without fusion. *Nat. Cell Biol.* **6**, 532-539.
Kennedy, S., Rettinger, S., Flye, M. W. and Ponder, K. P. (1995). Experiments in transgenic mice show that hepatocytes are the source for postnatal liver growth and do not stream. *Hepatology* **22**, 160-168.
Lagasse, E., Connors, H., Al-Dhalimy, M., Reitsma, M., Dohse, M., Osborne, L., Wang, X., Finegold, M., Weissman, I. L. and Grompe, M. (2000). Purified hematopoietic stem cells can differentiate into hepatocytes in vivo. *Nat. Med.* **6**, 1229-1234.
Lau, C., Thibodeaux, J. R., Hanson, R. G., Rogers, J. M., Grey, B. E., Stanton, M. E., Butenhoff, J. L. and Stevenson, L. A. (2003). Exposure to perfluorooctane sulfonate during pregnancy in rat and mouse. II: postnatal evaluation. *Toxicol. Sci.* **74**, 382-392.
Matsumoto, K., Yoshitomi, H., Rossant, J. and Zaret, K. S. (2001). Liver organogenesis promoted by endothelial cells prior to vascular function. *Science* **294**, 559-563.
Morris, L., Graham, C. F. and Gordon, S. (1991). Macrophages in haemopoietic and other tissues of the developing mouse detected by the monoclonal antibody F4/80. *Development* **112**, 517-526.
Morrison, S. J., Hemmati, H. D., Wandycz, A. M. and Weissman, I. L. (1995). The purification and characterization of fetal liver hematopoietic stem cells. *Proc. Natl. Acad. Sci. USA* **92**, 10302-10306.
Neufeld, D. S. (1997). Isolation of rat liver hepatocytes. *Methods Mol. Biol.* **75**, 145-151.
Nishikawa, S. I., Nishikawa, S., Kawamoto, H., Yoshida, H., Kizumoto, M., Kataoka, H. and Katsura, Y. (1998). In vitro generation of lymphohematopoietic cells from endothelial cells purified from murine embryos. *Immunity* **8**, 761-769.
Oettgen, P. (2001). Transcriptional regulation of vascular development. *Circ. Res.* **89**, 380-388.
Ogilvy, S., Metcalf, D., Gibson, L., Bath, M. L., Harris, A. W. and Adams, J. M. (1999). Promoter elements of vav drive transgene expression in vivo throughout the hematopoietic compartment. *Blood* **94**, 1855-1863.
Prost, S., Sheahan, S., Rannie, D. and Harrison, D. J. (2001). Adenovirus-mediated Cre deletion of floxed sequences in primary mouse cells is an efficient alternative for studies of gene deletion. *Nucleic Acids Res.* **29**, E80.
Recillas-Targa, F., Pikaart, M. J., Burgess-Beusse, B., Bell, A. C., Litt, M. D., West, A. G., Gaszner, M. and Felsenfeld, G. (2002). Position-effect protection and enhancer blocking by the chicken beta-globin insulator are separable activities. *Proc. Natl. Acad. Sci. USA* **99**, 6883-6888.
Sanchez, M. J., Holmes, A., Miles, C. and Dzierzak, E. (1996). Characterization of the first definitive hematopoietic stem cells in the AGM and liver of the mouse embryo. *Immunity* **5**, 513-525.
Sata, M., Saiura, A., Kunisato, A., Tojo, A., Okada, S., Tokuhisa, T., Hirai, H., Makuuchi, M., Hirata, Y. and Nagai, R. (2002). Hematopoietic stem cells differentiate into vascular cells that participate in the pathogenesis of atherosclerosis. *Nat. Med.* **8**, 403-409.
Shiojiri, N., Sano, M., Inujima, S., Nitou, M., Kanazawa, M. and Mori, M. (2000). Quantitative analysis of cell allocation during liver development, using the spf(ash)-heterozygous female mouse. *Am. J. Pathol.* **156**, 65-75.
Soriano, P. (1999). Generalized lacZ expression with the ROSA26 Cre reporter strain. *Nat. Genet.* **21**, 70-71.
Srinivas, S., Watanabe, T., Lin, C. S., William, C. M., Tanabe, Y., Jessell, T. M. and Costantini, F. (2001). Cre reporter strains produced by targeted insertion of EYFP and ECFP into the ROSA26 locus. *Dev. Biol.* **1**, 4.
Suzuki, A., Zheng, Y., Kondo, R., Kusakabe, M., Takada, Y., Fukao, K., Nakauchi, H. and Taniguchi, H. (2000). Flow-cytometric separation and enrichment of hepatic progenitor cells in the developing mouse liver. *Hepatology* **32**, 1230-1239.
Tamura, H., Okamoto, S., Iwatsuki, K., Futamata, Y., Tanaka, K., Nakayama, Y., Miyajima, A. and Hara, T. (2002). In vivo differentiation of stem cells in the aorta-gonad-mesonephros region of mouse embryo and adult bone marrow. *Exp. Hematol.* **30**, 957-966.
Wagers, A. J. and Weissman, I. L. (2004). Plasticity of adult stem cells. *Cell* **116**, 639-648.
Wang, X., Montini, E., Al-Dhalimy, M., Lagasse, E., Finegold, M. and Grompe, M. (2002). Kinetics of liver repopulation after bone marrow transplantation. *Am. J. Pathol.* **161**, 565-574.
Wei, J., Blum, S., Unger, M., Jarmy, G., Lamparter, M., Geishauser, A., Vlastos, G. A., Chan, G., Fischer, K. D., Rattat, D. et al. (2004). Embryonic endothelial progenitor cells armed with a suicide gene target hypoxic lung metastases after intravenous delivery. *Cancer Cell* **5**, 477-488.
Willenbring, H., Bailey, A. S., Foster, M., Akkari, Y., Dorrell, C., Olson, S., Finegold, M., Fleming, W. H. and Grompe, M. (2004). Myelomonocytic cells are sufficient for therapeutic cell fusion in liver. *Nat. Med.* **10**, 744-748.
Ye, M., Iwasaki, H., Laiosa, C. V., Stadtfeld, M., Xie, H., Heck, S., Clausen, B., Akashi, K. and Graf, T. (2003). Hematopoietic stem cells expressing the myeloid lysozyme gene retain long-term, multilineage repopulation potential. *Immunity* **19**, 689-699.
Yuan, R. H., Ogawa, D., Ogawa, E., Neufeld, D., Zhu, L., Shafritz, D. A. (2003). p27Kip1 inactivation provides a proliferative advantage to transplanted hepatocytes in DPPIV/Rag2 double knockout mice after repeated host liver injury. *Cell Transplant.* **12**, 907-919.
Zaret, K. S. (2002). Regulatory phases of early liver development: paradigms of organogenesis. *Nat. Rev. Genet.* **3**, 499-512.